Atmos. Chem. Phys. Discuss., https://doi.org/10.5194/acp-2019-5
Manuscript under review for journal Atmos. Chem. Phys.
Discussion started: 22 January 2019

Atmospheric Chemistry and Physics Discussions

Devastating Californian wildfires in November 2018 observed from space: the carbon monoxide perspective

Oliver Schneising, Michael Buchwitz, Maximilian Reuter, Heinrich Bovensmann, and John P. Burrows
Institute of Environmental Physics (IUP), University of Bremen FB1, Bremen, Germany
Correspondence: O. Schneising (oliver.schneising@iup.physik.uni-bremen.de)

Abstract. Due to proceeding climate change, some regions such as California are becoming warmer and drier entailing the risk that destructive wildfires and associated air pollution episodes continue to increase. November 2018 has turned into one of the most disastrous months in Californian history with two particularly destructive wildfires raging concurrently through the North and the South of the state leaving about $1000\,\mathrm{km}^2$ of land burnt to cinders. Both fires ignited at the wildland-urban interface causing at least 88 civilian fatalities and forcing the total evacuation of several cities and communities.

Here we demonstrate that the inherent carbon monoxide (CO) emissions of the wildfires and subsequent transport can be observed from space by analysing radiance measurements of the TROPOspheric Monitoring Instrument (TROPOMI) onboard the Sentinel-5 Precursor satellite in the shortwave infrared spectral range. From the determined CO distribution we assess the corresponding air quality burden in Californian major cities caused by the fires. As a result of the prevailing wind conditions, the largest CO load during the first days of the fires is found in Sacramento and San Francisco with city area averages exceeding boundary layer concentrations of $6\,\mathrm{mg\,m}^{-3}$ and $4\,\mathrm{mg\,m}^{-3}$, respectively. For some neighbourhoods in the northwest of Sacramento national ambient air quality standards ($10\,\mathrm{mg\,m}^{-3}$ with 8-hour averaging time) are likely exceeded.

1 Introduction

As a consequence of climate change, precipitation and temperature extremes in California during the cool season (October-May) are occurring more frequently with the dry periods becoming warmer and drier (Swain et al., 2016), which is associated with an increased fire risk. The wildfire season 2018 has been the most destructive on record with respect to burned land area, destroyed buildings, and death toll (California Department of Forestry and Fire Protection, 2018). After a series of blazes in July/August including the Mendocino Complex, the largest wildfire in Californian history, another round of large wildfires erupted in November, most prominently the Camp Fire and the Woolsey Fire.

The Camp Fire started in the morning of November 8 in Butte County in the North of the state and grew rapidly. It destroyed more than $600\,\mathrm{km}^2$ of land, almost 20000 structures, and caused 85 civilian fatalities. As a result, it became both California's most destructive and deadliest wildfire of all time. Several cities and communities had to be evacuated; the town of Paradise was wiped out by the fire.

Atmos. Chem. Phys. Discuss., https://doi.org/10.5194/acp-2019-5
Manuscript under review for journal Atmos. Chem. Phys.
Discussion started: 22 January 2019

Atmospheric Chemistry and Physics Discussions

The Woolsey Fire ignited on the same day as the Camp Fire in the early afternoon near the boundary between Los Angeles and Ventura counties. It burnt all the way to Malibu engulfing about $400\,\mathrm{km}^2$ of land, nearly 2000 structures, and killed three people. The fire forced the total evacuation of Bell Canyon, Malibu, and Oak Park – an unprecedented instance in history.

Smoke from the fires also reached the major cities of the state prompting health warnings and the advice to remain indoors or wear face masks in certain areas (Sacramento Metropolitan Air Quality Management District, 2018; Bay Area Air Quality Management District, 2018). The air quality was affected by particulate matter and carbon monoxide (CO), which results from the incomplete combustion of biomass during wildfires (Yurganov et al., 2005). CO is a colourless, odorless, and tasteless gas that is toxic in large concentrations because it combines with hemoglobin to carboxyhemoglobin, which cannot effectively transport oxygen anymore. It plays an important role in tropospheric chemistry being the leading sink of the hydroxyl radical (OH) and acting as a precursor to tropospheric ozone (The Royal Society, 2008).

The Environmental Protection Agency (EPA) is required to set National Ambient Air Quality Standards (NAAQS) for six pollutants considered harmful to public health and the environment, including carbon monoxide, by the Clean Air Act. The CO standards are fixed at $9\,\mathrm{ppm}$ ($10\,\mathrm{mg\,m^{-3}}$) with an 8-hour averaging time, and $35\,\mathrm{ppm}$ ($40\,\mathrm{mg\,m^{-3}}$) with a 1-hour averaging time, neither to be exceeded more than once per year (U.S. Environmental Protection Agency, 2011).

Up to now, the satellite-based analysis of CO emissions from fires was typically focused on midtropospheric CO data, e.g., from the Measurement of Pollution in the Troposphere (MOPITT) (Deeter et al., 2018), the Atmospheric Infrared Sounder (AIRS) (Fu et al., 2018), and the Infrared Atmospheric Sounding Interferometer (IASI) (Turquety et al., 2009) instruments, or upper-tropospheric CO data from the Microwave Limb Sounder (MLS) (Field et al., 2016). Nearly equal sensitivity to all altitude levels including the boundary layer, where fires are located, was taken advantage of by the Scanning Imaging Absorption Spectrometer for Atmospheric Chartography (SCIAMACHY) for cloud-free scenes (Buchwitz et al., 2007; Borsdorff et al., 2018b).

2 Data and Methods

In this study, we retrieve and analyse carbon monoxide from the radiance measurements of the TROPOspheric Monitoring Instrument (TROPOMI) onboard the Sentinel-5 Precursor (Sentinel-5P) satellite (Veefkind et al., 2012) using the latest version (v1.0) of the Weighting Function Modified DOAS (WFM-DOAS) algorithm (Buchwitz et al., 2006; Schneising et al., 2011, 2014) optimised to retrieve vertical columns of carbon monoxide and methane simultaneously (Schneising, 2017).

Sentinel-5P was launched in October 2017 into a sun-synchronous orbit with an equator crossing time of 1:30 p.m. local time. TROPOMI is a spaceborne nadir viewing imaging spectrometer measuring solar radiation reflected by the Earth in a push-broom configuration. It has a swath width of 2600 km on the Earth's surface and covers wavelength bands between the ultraviolet (UV) and the shortwave infrared (SWIR) combining a high spatial resolution with daily global coverage. The horizontal resolution of the TROPOMI nadir measurements, which depends on orbital position and spectral interval, is typically $7 \times 7\,\mathrm{km}^2$ for the SWIR bands used in this study. Due to its wide swath in conjunction with high spatial and temporal resolution, the observations of TROPOMI yield CO amounts and distributions with unprecedented level of detail on a global scale

Atmos. Chem. Phys. Discuss., https://doi.org/10.5194/acp-2019-5
Manuscript under review for journal Atmos. Chem. Phys.
Discussion started: 22 January 2019

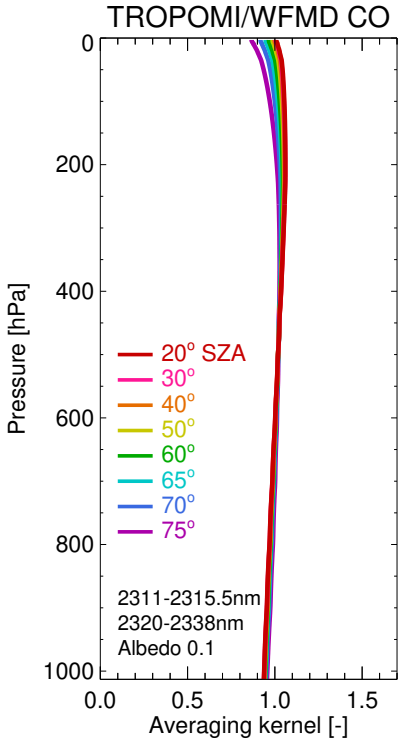

Figure 1. Column averaging kernels reflecting the altitude sensitivity of the retrievals.

(Borsdorff et al., 2018a). The heritage of the TROPOMI approach to retrieve CO and CH_4 comes from the SCIAMACHY project and its observations (Burrows et al., 1995; Bovensmann et al., 1999).

As a result of the observation of reflected solar radiation in the SWIR part of the solar spectrum, TROPOMI yields atmospheric carbon monoxide with high sensitivity to all altitude levels including the planetary boundary layer (see Figure 1) and is thus well suited to study emissions from fires. In order to convert the retrieved columns into mole fractions, they are divided by the corresponding dry air column obtained from the European Centre for Medium-Range Weather Forecasts (ECMWF) analysis. The resulting column-averaged dry air mole fractions are denoted by XCO.

Based on a validation with ground-based Fourier Transform Spectrometer (FTS) measurements of the Total Carbon Column Observing Network (TCCON) (Wunch et al., 2011), the TROPOMI/WFMD XCO data set is characterised by a random error (precision) of about 6 ppb and a systematic error (relative accuracy) of about 2 ppb (Van Roozendael et al., 2018).

For the present study a simple quality screening algorithm was implemented excluding measurements not sufficiently characterised by the forward model. It filters out measurements with a CO fit error larger than 10% or radiances in specific strong water vapour absorption bands (close to 2.4 µm) larger than 2.5 times the value, which one would expect for cloud-free scenes. For land covered cases, scenes with unrealistically low retrieved surface pressure (difference to ECMWF analysis larger than

Atmos. Chem. Phys. Discuss., https://doi.org/10.5194/acp-2019-5
Manuscript under review for journal Atmos. Chem. Phys.
Discussion started: 22 January 2019

Atmospheric Chemistry and Physics Discussions

300 hPa) are also excluded. As a consequence, high clouds are filtered out, while retrievals over low clouds may still be tolerated to some degree, thus increasing the number of utilisable scenes.

To get a visual impression of the smoke distribution originating from the fires, so-called true colour images (Red = Band I1, Green = Band M4, Blue = Band M3) from the Visible Infrared Imaging Radiometer Suite (VIIRS) instrument onboard the joint NASA/NOAA Suomi National Polar-orbiting Partnership (Suomi-NPP) satellite are used, which show land surface, oceanic and atmospheric features like the human eye would see them (Hillger et al., 2014).

The TROPOMI CO retrievals are also compared to the analysis of the ECMWF Integrated Forecasting System (IFS) provided by the Copernicus Atmosphere Monitoring Service (CAMS) (Inness et al., 2015), which assimilates MOPITT and IASI CO observations (Drummond et al., 2010; Clerbaux et al., 2009) and biomass-burning emissions from MACC's Global Fire Assimilation System (GFAS) (Kaiser et al., 2012).

To assess the CO burden in Californian major cities we compute the average total column enhancement (within 20 km radius around midtown, in units of mass per area) for the first days of the fire relative to November 7, which is considered as background. It is assumed that the additional CO from the fires is located in the well-mixed boundary layer, while the remaining upper part of the contaminated profile closely resembles the background profile, allowing to disentangle the near-surface abundances from the total column measurements. To this end, the total column enhancement is divided by the boundary layer height obtained from the ECMWF analysis to get the boundary layer concentration anomaly due to the fires (in units of mass per volume). The areal variation (1σ) of this anomaly is determined from the standard deviations of the CO columns measuring the inhomogeneity of the boundary layer concentrations within the respective city area.

3 Results

As a result of the Camp and Woolsey fires ignited on November 8, associated smoke overcast large parts of the state for days. This can clearly be seen on the VIIRS true colour images in Figure 2. Sentinel-5 Precursor and Suomi-NPP fly in loose formation, with Sentinel-5P trailing behind by 3.5 minutes, ensuring that both satellites observe (almost) the same scene. Thus, the corresponding images can be compared directly. Figure 3 shows the XCO distribution over California, which obviously matches the smoke emission and transport patterns detected by VIIRS unambiguously. This substantiates that the observed CO enhancements are actually originating from the wildfires.

It is important to note that it can be excluded that the satellite-derived statewide CO column enhancement is only an artefact as a result of light path lengthening because of aerosol scattering at the particulate matter of the smoke. This is verified by the fact that the simultaneously retrieved gases, methane and water vapour, are not considerably increased compared to the pre-fire background abundances; light path related systematic errors would affect all retrieved gases similarly.

For comparison, Figure 4 shows the CAMS near-real-time CO analysis on a $0.75° \times 0.75°$ grid for the same days shown in the previous figures close to the time of the TROPOMI overpass. Although CO emissions from the fires are obviously included in the CAMS data, the transport patterns and intensity distribution seem to be somewhat different, e.g., abundances on November

Atmos. Chem. Phys. Discuss., https://doi.org/10.5194/acp-2019-5
Manuscript under review for journal Atmos. Chem. Phys.
Discussion started: 22 January 2019

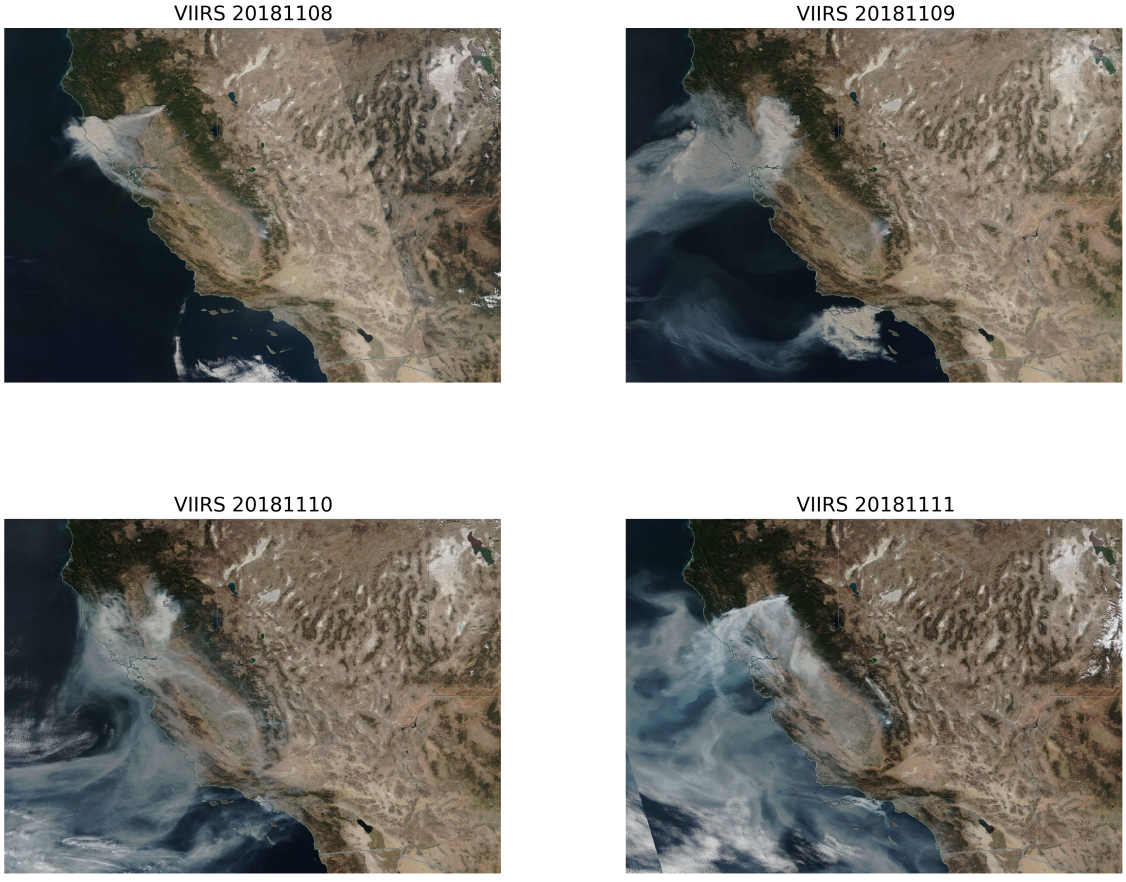

Figure 2. True colour reflectances from the Visible Infrared Imaging Radiometer Suite (VIIRS) for the first days of the fires taken from the NASA Worldview application.

11 are predicted to be considerably larger than measured by the satellite, whereas they are predicted to be considerably smaller on November 8.

Averaged boundary layer concentration anomalies of CO (relative to November 7) in major Californian cities during the first days of the Camp and Woolsey fires are presented in Table 1. The largest values were found for Sacramento and San Francisco on November 9 and 10, due to the prevailing wind conditions, exceeding concentrations of $6\,\mathrm{mg\,m^{-3}}$ and $4\,\mathrm{mg\,m^{-3}}$, respectively, which is about half of the national CO air quality standard of $10\,\mathrm{mg\,m^{-3}}$. The cities in the South of the state are less affected owed to more favorable weather conditions.

Although the Sacramento and San Francisco city averages are compliant with air quality standards, the large associated variations indicate an uneven CO distribution within both towns, in particular for Sacramento. This interpretation is supported by the CO distribution depicted in Figure 3 showing that the plume's edge of the Camp Fire is located near Sacramento leading to a larger burden in the northwest compared to the rest of the city.

Atmos. Chem. Phys. Discuss., https://doi.org/10.5194/acp-2019-5
Manuscript under review for journal Atmos. Chem. Phys.
Discussion started: 22 January 2019

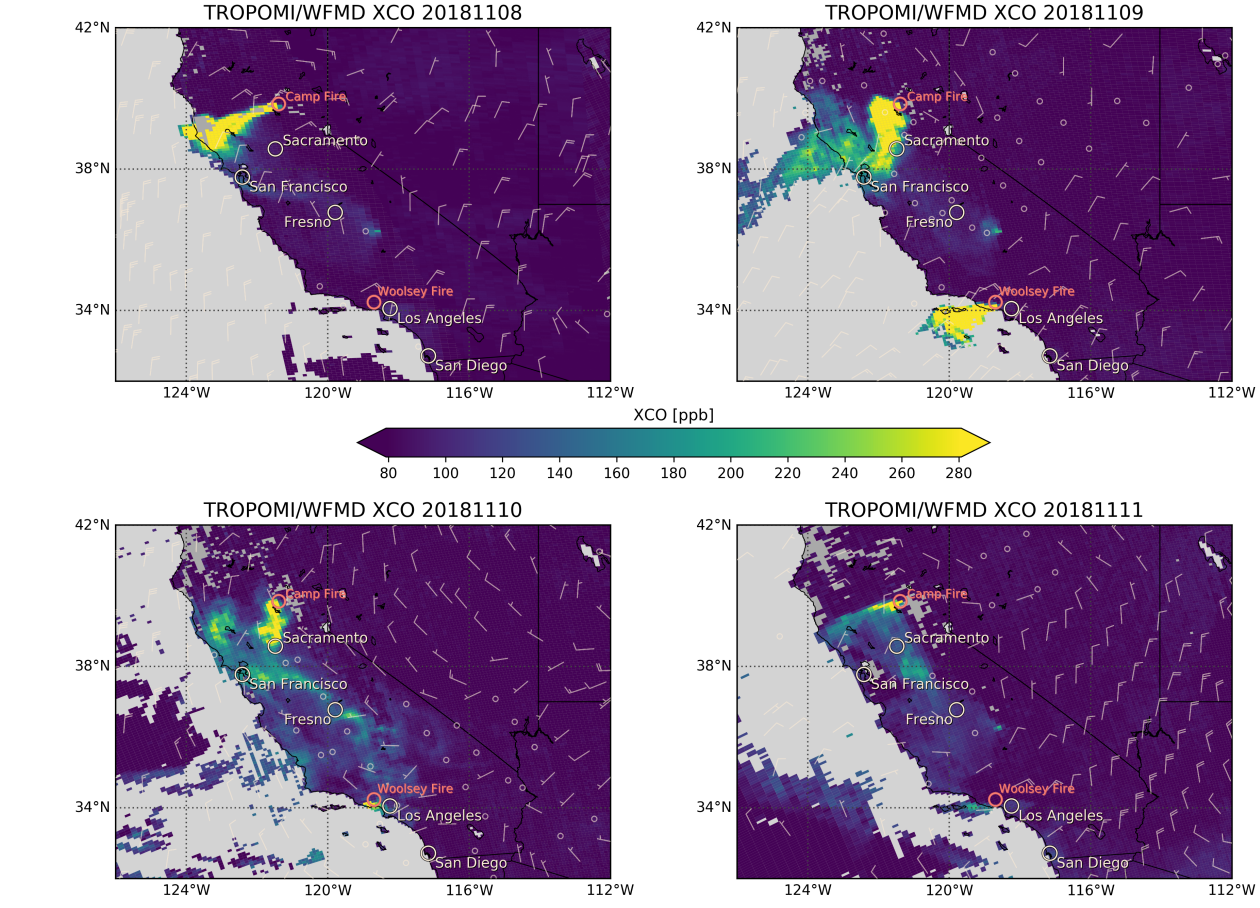

Figure 3. Retrieved carbon monoxide column-averaged mole fractions from TROPOMI for the same days as in Figure 2. Also shown is the mean wind in the boundary layer obtained from ECMWF data.

Table 1. Averaged boundary layer concentration anomaly of CO (relative to November 7) and associated areal variation (1σ) in major Californian cities during the first days of the Camp and Woolsey fires.

	November 8 [mg m^{-3}]	November 9 [mg m^{-3}]	November 10 [mg m^{-3}]	November 11 [mg m^{-3}]
Sacramento	0.21 ± 0.04	4.80 ± 2.25	6.64 ± 3.93	1.43 ± 0.15
San Francisco	0.67 ± 0.23	4.14 ± 0.86	3.99 ± 0.94	0.57 ± 0.19
Fresno	0.26 ± 0.05	0.60 ± 0.15	2.02 ± 0.28	1.10 ± 0.20
Los Angeles	0.32 ± 0.05	0.15 ± 0.09	1.43 ± 0.89	0.43 ± 0.09
San Diego	0.42 ± 0.07	0.25 ± 0.09	0.23 ± 0.09	0.99 ± 0.13

Atmos. Chem. Phys. Discuss., https://doi.org/10.5194/acp-2019-5
Manuscript under review for journal Atmos. Chem. Phys.
Discussion started: 22 January 2019

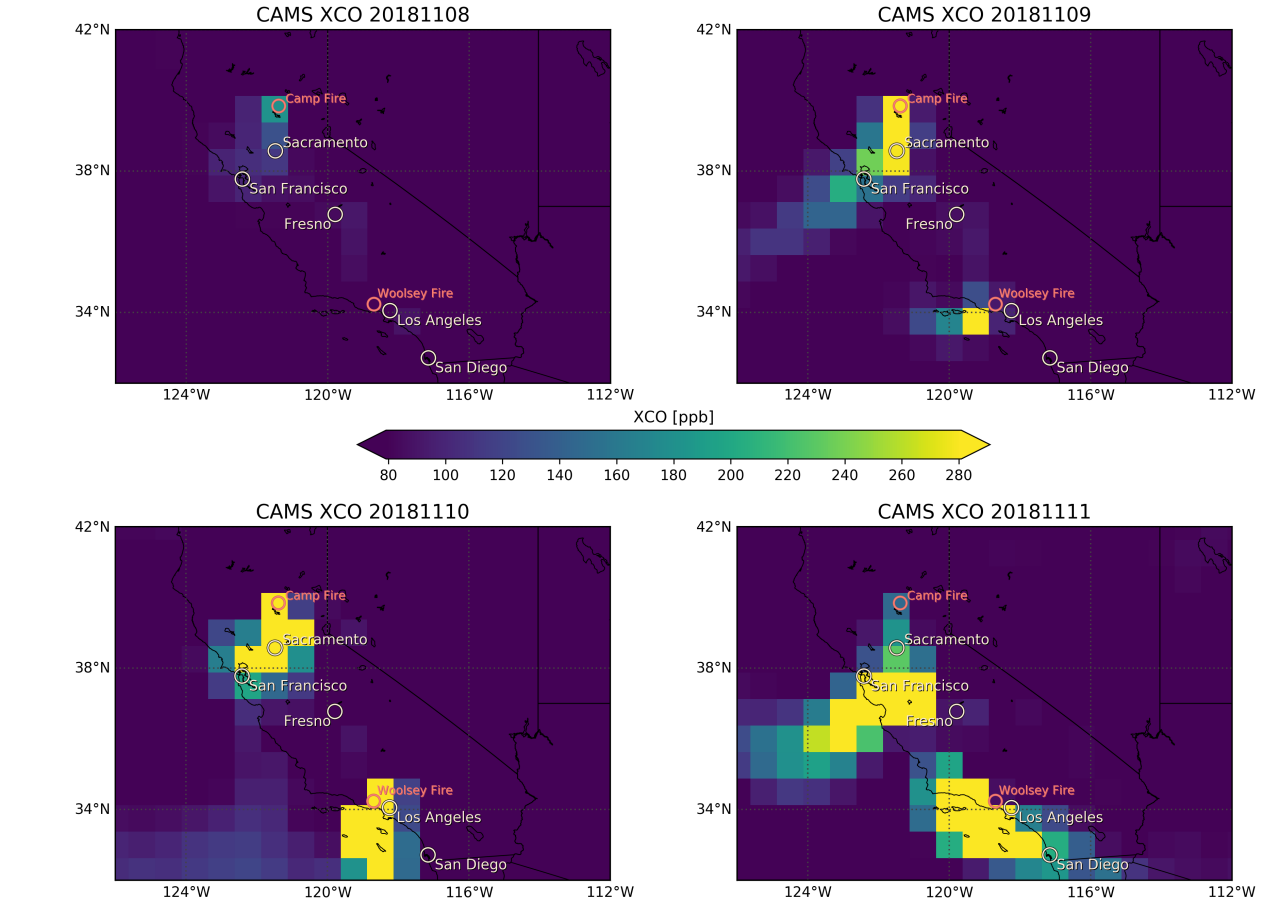

Figure 4. CAMS near-real time CO analysis for the first days of the fires at 9 p.m. UTC (Coordinated Universal Time) corresponding to 1 p.m. local time (Pacific Standard Time).

The largest total column value within all city radii is actually found on November 10 near Sacramento International Airport. The corresponding spectral fit is shown in Figure 5 demonstrating a massive CO load and that the fit residual is small relative to the individual scaled derivatives (weighting functions) with respect to all fit parameters including the weak CO absorption. When compared to a nearby background scene from November 7 (see Figure 6), one finds a considerable column enhancement of $3.0\,\mathrm{g\,m^{-2}}$. Given the ECMWF analysis boundary layer height of $171\,\mathrm{m}$, this corresponds to a boundary layer concentration anomaly of $17.5\,\mathrm{mgCO\,m^{-3}}$. The corresponding enhancement on November 9 at the same location was $2.1\,\mathrm{g\,m^{-2}}$ with a boundary layer height of $266\,\mathrm{m}$ leading to a boundary layer concentration anomaly of $7.9\,\mathrm{mgCO\,m^{-3}}$. Thus, it is reasonable to assume that the national ambient air quality standard of $10\,\mathrm{mgCO\,m^{-3}}$ was likely exceeded for at least one 8-hour average in some neighbourhoods in the northwest of Sacramento.

To further assess the described area with significantly increased boundary layer concentrations, we revisit the discussed contaminated scene near Sacramento International Airport on November 10 and analyse associated results from CAMS and

Atmos. Chem. Phys. Discuss., https://doi.org/10.5194/acp-2019-5
Manuscript under review for journal Atmos. Chem. Phys.
Discussion started: 22 January 2019

Atmospheric Chemistry and Physics Discussions

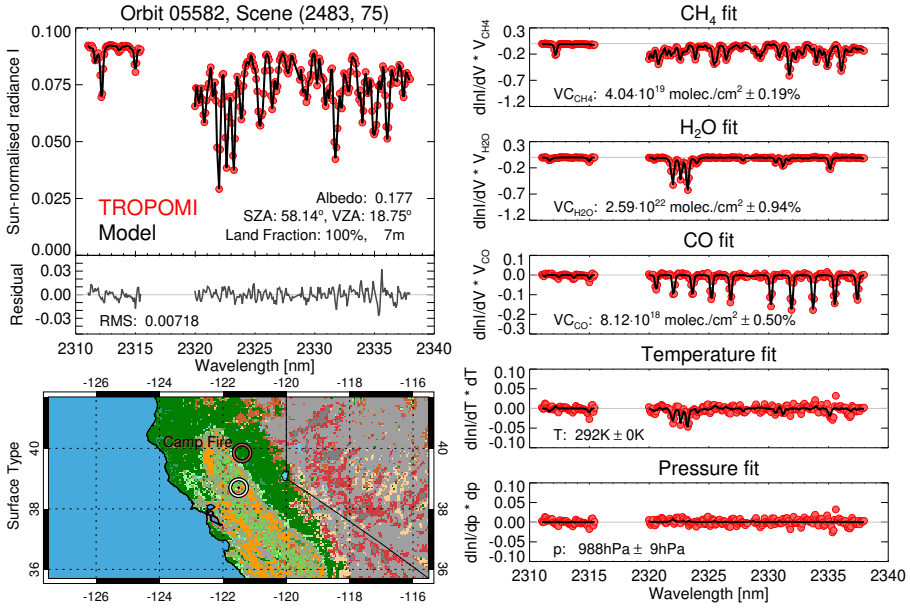

Figure 5. Example spectral fit for a contaminated scene (white circle on the map) on November 10 near Sacramento International Airport. The different colours on the map represent different surface types (United States Geological Survey, 2018). On the left, the measured sun-normalised radiance (red), the fitted WFM-DOAS linearised radiative transfer model (black), and the resulting fit residual are shown. The right-hand panels compare the sum (red) of scaled derivative and fit residual to the scaled derivative itself (black) for each fit parameter. The fit residual is considered small because the red symbols follow the spectral features of the respective black line.

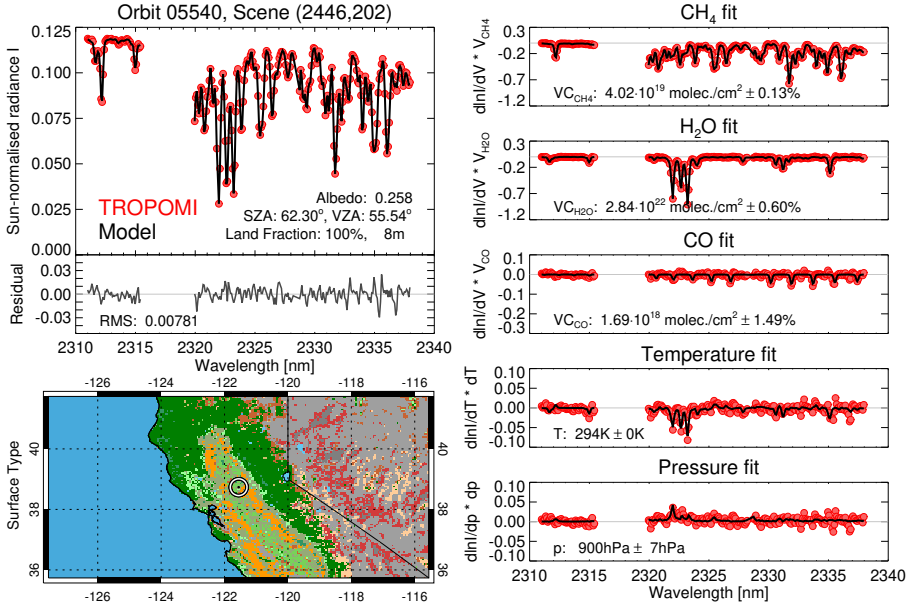

Figure 6. Background scene on November 7 for the contaminated scene near Sacramento International Airport shown in Figure 5.

Atmos. Chem. Phys. Discuss., https://doi.org/10.5194/acp-2019-5
Manuscript under review for journal Atmos. Chem. Phys.
Discussion started: 22 January 2019

Atmospheric Chemistry and Physics Discussions

ground-based Quality Assurance Air Monitoring Site Information. For the grid-box comprising the mentioned satellite scene, CAMS predicts an even larger column enhancement of $7.0\,\mathrm{g\,m^{-2}}$ corresponding to a boundary layer concentration anomaly of $34.4\,\mathrm{mgCO\,m^{-3}}$ (boundary layer height of $202\,\mathrm{m}$ according to the ECMWF analysis). However, the scene is located near the bottom edge of the rather large CAMS grid-box expanding further north in the direction of the fire origin. This potentially explains the large boundary layer concentration.

Ground-based measurements are available from the Air Quality and Meteorological Information System (AQMIS) network (California Air Resources Board, 2018). Unfortunately, there are only two CO measurement sites in Sacramento County and data for November 2018 has to be considered preliminary. For the site at Bercut Drive in Sacramento most of the data is missing during the first days of the fire. The second site at Blackfoot Way in North Highlands is located farther north and closer to the analysed contaminated satellite scene. This site also exhibits large data gaps for the analysed time period. On November 10, 50% of the hourly data are missing reducing the significance of the daily maximum 1-hour average value, which is stated to be $4\,\mathrm{ppm}$ ($4.6\,\mathrm{mgCO\,m^{-3}}$).

Figure 7 shows the boundary layer concentration anomalies of Sacramento and its surrounding districts allowing to get an overview of the situation by highlighting the locations of the different measurements. As can be seen, the AQMIS site is located easterly of the satellite scene with maximal city area CO value, where concentrations are beginning to decline steeply. The corresponding satellite average for the North Highlands site is estimated to be $6.28 \pm 2.72\,\mathrm{mgCO\,m^{-3}}$, which is broadly consistent with the maximal daily value of the ground-based measurements.

4 Conclusions

The local CO emissions of Californian wildfires and subsequent transport can be clearly observed from space. This is a demonstration of the unprecedented capabilities concerning level of detail modern wide-swath imaging satellite instruments offer. As large sources are readily detected in a single overpass, new fields of application are enabled, in particular the detection of emission hot spots or air quality monitoring tasks. The assessment of the air quality burden in Californian major cities during the first days of the Camp Fire and Woolsey Fire can be thought of as an initial step in this direction.

The analysed fires were the latest episodes of the deadliest and most destructive wildfire season the state of California has ever faced. Increasing unusual weather conditions with dryness of vegetation on the rise bring deadly fires and associated air pollution forward. The increasing number of people living in the wildland-urban interface paired with proceeding climate change entailing longer lasting and more intense fire seasons temper the outlook for the future (Radeloff et al., 2018). Countermeasures with respect to forest management or building practices and mitigation of climate change will be key challenges of the century to prevent that fatal blazes and air quality decline establish as the new normal in the Western United States or other wildfire regions.

Atmos. Chem. Phys. Discuss., https://doi.org/10.5194/acp-2019-5
Manuscript under review for journal Atmos. Chem. Phys.
Discussion started: 22 January 2019

Atmospheric Chemistry and Physics Discussions

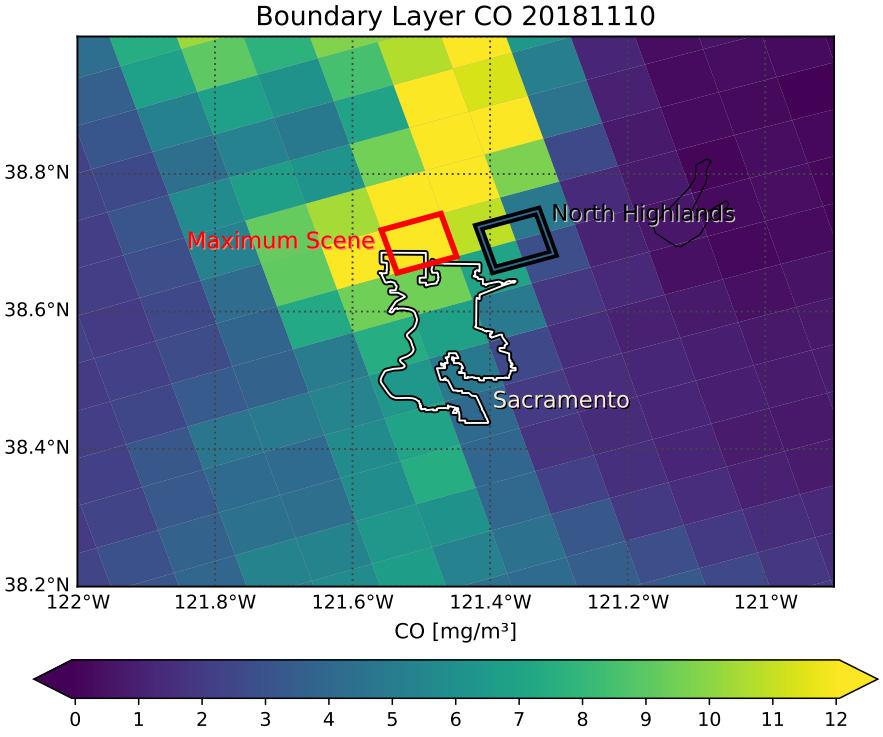

Figure 7. Boundary layer concentration anomalies of Sacramento and its environs determined from TROPOMI CO total column measurements and boundary layer heights from the ECMWF analysis. Highlighted are the satellite scene with maximal city area value ($17.5\,\mathrm{mgCO\,m^{-3}}$, red) and the location of the AQMIS site in North Highlands (black). The maximum 1-hour average value of the ground-based site ($4.6\,\mathrm{mgCO\,m^{-3}}$) is colour-coded within the black frame; the corresponding satellite average is estimated to be $6.28 \pm 2.72\,\mathrm{mgCO\,m^{-3}}$.

Data availability. The carbon monoxide data set presented in this publication can be accessed via http://www.iup.uni-bremen.de/carbon_ghg/public_data/tropomi_201811_ca/.

Author contributions. OS: writing the paper, design and operation of the satellite retrievals, data analysis, interpretation. MB, MR, HB, JPB: significant conceptual input to writing, design of the satellite retrievals, interpretation.

Competing interests. The authors declare that they have no conflict of interest.

Acknowledgements. The research leading to these results has in part been funded by the ESA projects GHG-CCI and S5L2PP, the Federal Ministry of Education and Research project AIRSPACE, and by the State and the University of Bremen.

Sentinel-5 Precursor is an ESA mission implemented on behalf of the European Commission. The TROPOMI payload is a joint development by ESA and the Netherlands Space Office (NSO). The Sentinel-5 Precursor ground-segment development has been funded by ESA and with national contributions from The Netherlands, Germany, and Belgium.

We acknowledge the use of VIIRS imagery from the NASA Worldview application (https://worldview.earthdata.nasa.gov/) operated by the NASA/Goddard Space Flight Center Earth Science Data and Information System (ESDIS) project, the use of data from the California Department of Forestry and Fire Protection and the U.S. Environmental Protection Agency. We also thank the European Centre for Medium-Range Weather Forecasts (ECMWF) for providing the meteorological analysis and the Copernicus Atmosphere Monitoring Service (CAMS) carbon monoxide data. Ground-based CO data was obtained using the Air Quality Data (PST) Query Tool (https://www.arb.ca.gov/aqmis2/aqmis2.php) of the Air Quality and Meteorological Information System (AQMIS).

References

Bay Area Air Quality Management District: A Winter Spare the Air Alert is being called through Monday, November 12, due to smoke impacts from the Butte County fire, Press Release, November 9, http://www.baaqmd.gov/~/media/files/communications-and-outreach/publications/news-releases/2018/wsta_181109_2018_092-pdf.pdf, 2018.

Borsdorff, T., aan de Brugh, J., Hu, H., Hasekamp, O., Sussmann, R., Rettinger, M., Hase, F., Gross, J., Schneider, M., Garcia, O., Stremme, W., Grutter, M., Feist, D. G., Arnold, S. G., De Mazière, M., Kumar Sha, M., Pollard, D. F., Kiel, M., Roehl, C., Wennberg, P. O., Toon, G. C., and Landgraf, J.: Mapping carbon monoxide pollution from space down to city scales with daily global coverage, Atmos. Meas. Tech., 11, 5507–5518, https://doi.org/10.5194/amt-11-5507-2018, 2018a.

Borsdorff, T., Andrasec, J., aan de Brugh, J., Hu, H., Aben, I., and Landgraf, J.: Detection of carbon monoxide pollution from cities and wildfires on regional and urban scales: the benefit of CO column retrievals from SCIAMACHY 2.3 μm measurements under cloudy conditions, Atmos. Meas. Tech., 11, 2553–2565, https://doi.org/10.5194/amt-11-2553-2018, 2018b.

Bovensmann, H., Burrows, J. P., Buchwitz, M., Frerick, J., Noël, S., Rozanov, V. V., Chance, K. V., and Goede, A. P. H.: SCIAMACHY – Mission Objectives and Measurement Modes, J. Atmos. Sci., 56, 127–150, https://doi.org/10.1175/1520-0469(1999)056<0127:SMOAMM>2.0.CO;2, 1999.

Buchwitz, M., de Beek, R., Noël, S., Burrows, J. P., Bovensmann, H., Schneising, O., Khlystova, I., Bruns, M., Bremer, H., Bergamaschi, P., Körner, S., and Heimann, M.: Atmospheric carbon gases retrieved from SCIAMACHY by WFM-DOAS: version 0.5 CO and CH_4 and impact of calibration improvements on CO_2 retrieval, Atmos. Chem. Phys., 6, 2727–2751, https://doi.org/10.5194/acp-6-2727-2006, 2006.

Buchwitz, M., Khlystova, I., Bovensmann, H., and Burrows, J. P.: Three years of global carbon monoxide from SCIAMACHY: comparison with MOPITT and first results related to the detection of enhanced CO over cities, Atmos. Chem. Phys., 7, 2399–2411, https://doi.org/10.5194/acp-7-2399-2007, 2007.

Burrows, J. P., Hölzle, E., Goede, A. P. H., Visser, H., and Fricke, W.: SCIAMACHY – Scanning Imaging Absorption Spectrometer for Atmospheric Chartography, Acta Astronautica, 35, 445–451, https://doi.org/10.1016/0094-5765(94)00278-T, 1995.

California Air Resources Board: Air Quality and Meteorological Information System, https://www.arb.ca.gov/aqmis2/aqmis2.php, 2018.

California Department of Forestry and Fire Protection: Statistics and Events, http://cdfdata.fire.ca.gov/incidents/incidents_statsevents, 2018.

Clerbaux, C., Boynard, A., Clarisse, L., George, M., Hadji-Lazaro, J., Herbin, H., Hurtmans, D., Pommier, M., Razavi, A., Turquety, S., Wespes, C., and Coheur, P.-F.: Monitoring of atmospheric composition using the thermal infrared IASI/MetOp sounder, Atmos. Chem. Phys., 9, 6041–6054, https://doi.org/10.5194/acp-9-6041-2009, 2009.

Deeter, M. N., Martinez-Alonso, S., Andreae, M. O., and Schlager, H.: Satellite-Based Analysis of CO Seasonal and Interannual Variability Over the Amazon Basin, J. Geophys. Res., 123, 5641–5656, 2018.

Drummond, J. R., Zou, J., Nichitiu, F., Kar, J., Deschambaut, R., and Hackett, J.: A review of 9-year performance and operation of the MOPITT instrument, Adv. Space Res., 45, 760–774, https://doi.org/10.1016/j.asr.2009.11.019, 2010.

Field, R. D., van der Werf, G. R., Fanin, T., Fetzer, E. J., Fuller, R., Jethva, H., Levy, R., Livesey, N. J., Luo, M., Torres, O., and Worden, H. M.: Indonesian fire activity and smoke pollution in 2015 show persistent nonlinear sensitivity to El Niño-induced drought, Proc. Natl. Acad. Sci. USA, 113, 9204–9209, https://doi.org/10.1073/pnas.1524888113, 2016.

Fu, Y., Li, R., Huang, J., Bergeron, Y., Fu, Y., Wang, Y., and Gao, Z.: Satellite-Observed Impacts of Wildfires on Regional Atmosphere Composition and the Shortwave Radiative Forcing: A Multiple Case Study, J. Geophys. Res., 123, 8326–8343, 2018.

Hillger, D., Seaman, C., Liang, C., Miller, S., Lindsey, D., and Kopp, T.: Suomi NPP VIIRS Imagery evaluation, J. Geophys. Res.: Atmospheres, 119, 6440–6455, https://doi.org/10.1002/2013JD021170, 2014.

Inness, A., Blechschmidt, A.-M., Bouarar, I., Chabrillat, S., Crepulja, M., Engelen, R. J., Eskes, H., Flemming, J., Gaudel, A., Hendrick, F., Huijnen, V., Jones, L., Kapsomenakis, J., Katragkou, E., Keppens, A., Langerock, B., de Mazière, M., Melas, D., Parrington, M., Peuch, V. H., Razinger, M., Richter, A., Schultz, M. G., Suttie, M., Thouret, V., Vrekoussis, M., Wagner, A., and Zerefos, C.: Data assimilation of satellite-retrieved ozone, carbon monoxide and nitrogen dioxide with ECMWF's Composition-IFS, Atmos. Chem. Phys., 15, 5275–5303, https://doi.org/10.5194/acp-15-5275-2015, 2015.

Kaiser, J. W., Heil, A., Andreae, M. O., Benedetti, A., Chubarova, N., Jones, L., Morcrette, J.-J., Razinger, M., Schultz, M. G., Suttie, M., and van der Werf, G. R.: Biomass burning emissions estimated with a global fire assimilation system based on observed fire radiative power, Biogeosciences, 9, 527–554, https://doi.org/10.5194/bg-9-527-2012, 2012.

Radeloff, V. C., Helmers, D. P., Kramer, H. A., Mockrin, M. H., Alexandre, P. M., Bar-Massada, A., Butsic, V., Hawbaker, T. J., Martinuzzi, S., Syphard, A. D., and Stewart, S. I.: Rapid growth of the US wildland-urban interface raises wildfire risk, Proc. Natl. Acad. Sci. USA, 115, 3314–3319, https://doi.org/10.1073/pnas.1718850115, 2018.

Sacramento Metropolitan Air Quality Management District: Smoke Health Statement Due to Camp Fire, Press Release, November 9, http://www.airquality.org/Communications/Documents/SmokeHealthStatement_CampFire_110918_2.docx.pdf, 2018.

Schneising, O.: Sentinel-5 Precursor methane: Retrieval, comparisons and interpretation (S5PCH4), Technical Report ESA project GHG-CCI, 2017.

Schneising, O., Buchwitz, M., Reuter, M., Heymann, J., Bovensmann, H., and Burrows, J. P.: Long-term analysis of carbon dioxide and methane column-averaged mole fractions retrieved from SCIAMACHY, Atmos. Chem. Phys., 11, 2863–2880, https://doi.org/10.5194/acp-11-2863-2011, 2011.

Schneising, O., Burrows, J. P., Dickerson, R. R., Buchwitz, M., Reuter, M., and Bovensmann, H.: Remote sensing of fugitive methane emissions from oil and gas production in North American tight geologic formations, Earth's Future, 2, 548–558, https://doi.org/10.1002/2014EF000265, 2014.

Swain, D. L., Horton, D. E., Singh, D., and Diffenbaugh, N. S.: Trends in atmospheric patterns conducive to seasonal precipitation and temperature extremes in California, Science Advances, 2, e1501344, https://doi.org/10.1126/sciadv.1501344, 2016.

The Royal Society: Ground-level ozone in the 21st century: future trends, impacts and policy implications, Science Policy Report 15/08, https://royalsociety.org/~/media/Royal_Society_Content/policy/publications/2008/7925.pdf, 2008.

Turquety, S., Hurtmans, D., Hadji-Lazaro, J., Coheur, P.-F., Clerbaux, C., Josset, D., and Tsamalis, C.: Tracking the emission and transport of pollution from wildfires using the IASI CO retrievals: analysis of the summer 2007 Greek fires, Atmos. Chem. Phys., 9, 4897–4913, https://doi.org/10.5194/acp-9-4897-2009, 2009.

United States Geological Survey: Land Cover Products – Global Land Cover Characterization (GLCC), https://www.usgs.gov/centers/eros/science/usgs-eros-archive-land-cover-products-global-land-cover-characterization-glcc, 2018.

U.S. Environmental Protection Agency: National Ambient Air Quality Standards (NAAQS) for Carbon Monoxide (CO), Federal Register: 76 FR 54293, http://www.gpo.gov/fdsys/pkg/FR-2011-08-31/pdf/2011-21359.pdf, 2011.

Van Roozendael et al.: Sentinel 5 L2 Prototype Processors: Scientific Verification Report, Technical Report ESA project S5L2PP, 2018.

Veefkind, J. P., Aben, I., McMullan, K., Förster, H., de Vries, J., Otter, G., Claas, J., Eskes, H. J., de Haan, J. F., Kleipool, Q., van Weele, M., Hasekamp, O., Hoogeveen, R., Landgraf, J., Snel, R., Tol, P., Ingmann, P., Voors, R., Kruizinga, B., Vink, R., Visser, H., and Levelt,

P. F.: TROPOMI on the ESA Sentinel-5 Precursor: A GMES mission for global observations of the atmospheric composition for climate, air quality and ozone layer applications, Remote Sensing of Environment, 120, 70–83, https://doi.org/10.1016/j.rse.2011.09.027, 2012.

Wunch, D., Toon, G. C., Blavier, J.-F. L., Washenfelder, R. A., Notholt, J., Connor, B. J., Griffith, D. W. T., Sherlock, V., and Wennberg, P. O.: The Total Carbon Column Observing Network, Phil. Trans. R. Soc. A, 369, 2087–2112, https://doi.org/10.1098/rsta.2010.0240, 2011.

Yurganov, L. N., Duchatelet, P., Dzhola, A. V., Edwards, D. P., Hase, F., Kramer, I., Mahieu, E., Mellqvist, J., Notholt, J., Novelli, P. C., Rockmann, A., Scheel, H. E., Schneider, M., Schulz, A., Strandberg, A., Sussmann, R., Tanimoto, H., Velazco, V., Drummond, J. R., and Gille, J. C.: Increased Northern Hemispheric carbon monoxide burden in the troposphere in 2002 and 2003 detected from the ground and from space, Atmos. Chem. Phys., 5, 563–573, https://doi.org/10.5194/acp-5-563-2005, 2005.